Rostaniha 26(1): 27–48 (2025) – Research Article

رستنیها ۲۶(۱): ۴۸–۲۷ (۱۴۰۴) – مقاله پژوهشی

DOI: 10.22092/bot.j.iran.2025.369416.1420

In Silico genomic fingerprints of the pathogenic cyanobacterial strains isolated from Alma-Gol Wetland (Golestan Province, Iran), using highly repeated sequences

Received: 09.05.2025 ========== Revised: 06.07.2025 ========== Accepted: 15.07.2025

Marzieh Samadi: MSc Student, Department of Biology, SR.C., Islamic Azad University, Tehran, Iran

Hassan Beiranvand: MSc Student, Department of Biology, SR.C., Islamic Azad University, Tehran, Iran

Morteza Mohajeri Amiri: Assistant Prof., Department of Biology, SR.C., Islamic Azad University, Tehran, Iran

Bahareh Nowruzi✉: Associate Prof., Department of Biology, SR.C., Islamic Azad University, Tehran, Iran (bahare77biol@gmail.com)

Abstract

Alma-Gol Wetland (Golestan Province, Iran) is a permanent habitat for the cultivation of many fish and aquatic organisms and is a popular destination for many travelers during the warm seasons of the year. The discovery of several dead fish carcasses on the water surface indicated the presence of cyanotoxins in the said area. Therefore, the present study, is aimed to screen potentially toxic cyanobacterial strains in this wetland by amplifying *mcyG*, *mcyD*, and *mcyE* toxic genes, as well as structural genes including 16S rRNA and ITS. It was also employed the rep-PCR technique to amplify highly repetitive genes HIP, STRR, and ERIC. The results obtained from the dendrogram based on the amplification of palindromic primers showed that, strains *Nostoc* sp. 9, *Aliinostoc* sp. 1, and *Desmonostoc* sp. 10 clustered together, while strains *Calothrix* sp. 7 and *Neowestiellopsis* sp. 2 mostly formed separate branches. However, only the strain *Neowestiellopsis* sp. 2 contained the toxic gene *mcyD*. Furthermore, comparative analysis of the ITS region length revealed that, both the length and the structure of the D1-D1 and BOX B helices differed from those of other strains. This study is among the first to demonstrate that fingerprinting techniques can provide new insights into different cyanobacterial strains.

Keywords: Dendrogram, molecular phylogeny, palindromic primers, phylogenetic tree, toxic cyanobacteria

مطالعه انگشت‌نگاری ژنومی درون‌رایانه‌ای سویه‌های سیانوباکتریایی بیماری‌زا جداشده از تالاب آلماگل (استان گلستان) با استفاده از توالی‌های به شدت تکراری

دریافت: ۱۴۰۴/۰۲/۱۹ ========== بازنگری: ۱۴۰۴/۰۴/۱۵ ========== پذیرش: ۱۴۰۴/۰۴/۲۴

مرضیه صمدی: دانشجوی کارشناسی ارشد بخش زیست‌شناسی، واحد علوم و تحقیقات، دانشگاه آزاد اسلامی، تهران، ایران

حسن بیرانوند: دانشجوی کارشناسی ارشد بخش زیست‌شناسی، واحد علوم و تحقیقات، دانشگاه آزاد اسلامی، تهران، ایران

مرتضی مهاجری امیری: استادیار بخش زیست‌شناسی، واحد علوم و تحقیقات، دانشگاه آزاد اسلامی، تهران، ایران

بهاره نوروزی✉: دانشیار بخش زیست‌شناسی، واحد علوم و تحقیقات، دانشگاه آزاد اسلامی، تهران، ایران (bahare77biol@gmail.com)

خلاصه

تالاب آلماگل (استان گلستان)، محل دایمی پرورش بسیاری از ماهی‌ها و موجودات آبزی، محل بازدید عمومی بسیاری از گردشگران در فصول گرم سال است. شناسایی اجساد مرده چندین ماهی روی سطح آب نشان از حضور سیانوباکتری‌های بیماری‌زا (سیانوتوکسین‌ها) در این منطقه بود. به همین دلیل در تحقیق حاضر، با تکثیر ژن‌های بیماری‌زای *mcyG*، *mcyD* و *mcyE* و همچنین ژن‌های ساختاری از جمله 16S rRNA و ITS به همراه استفاده از روش rep-PCR برای تکثیر ژن‌های به شدت تکراری HIP، STRR و ERIC، به غربالگری سویه بالقوه سیانوباکتری‌های بیماری‌زای این تالاب پرداخته شد. نتایج به دست آمده از دندروگرام حاصل از تکثیر پرایمرهای پالیندرومیک نشان داد سویه‌های *Nostoc* sp. 9، *Aliinostoc* sp. 1 و *Desmonostoc* sp. 10 در کلاد مشترک و سویه‌های *Calothrix* sp. 7 و *Neowestiellopsis* sp. 2 در بیشتر موارد، انشعابات جداگانه‌ای را تشکیل دادند. با این حال، تنها سویه *Neowestiellopsis* sp. 2 حاوی ژن بیماری‌زای *mcyD* بود. همچنین، نتایج حاصل از آنالیز مقایسه طول مناطق ITS نشان داد که طول منطقه و همچنین ساختار مارپیچ‌های D1-D1 و BOX B با سایر سویه‌ها متفاوت بود. مطالعه حاضر جزو نخستین تحقیقات انجام شده است که نشان داد می‌توان با استفاده از روش انگشت‌نگاری، اطلاعات جدیدی را در زمینه سویه‌های مختلف سیانوباکتری ارایه نمود.

واژه‌های کلیدی: پرایمرهای پالیندرومیک، درخت فیلوژنتیک، دندروگرام، سیانوباکتری‌های سمی، فیلوژنی مولکولی

Introduction

Cyanobacteria are a group of ancient photosynthetic microorganisms considered among the earliest oxygen-producing life forms on earth. They play a major role in shaping early ecosystems and driving biological evolution. Despite being prokaryotic organisms and sharing structural similarities with other bacteria, cyanobacteria exhibit several functional characteristics akin to higher plants, particularly their ability to perform oxygenic photosynthesis and produce oxygen. Their significance extends beyond ecological contributions; in recent decades, considerable attention has been directed toward their biotechnological potential, especially in pharmaceuticals, and agriculture (Sánchez-Baracaldo *et al*. 2022).

Cyanobacteria produce a wide array of biologically active secondary metabolites, many of which exhibit antimicrobial, antifungal, cytotoxic, and antitumor properties (Nowruzi & Beiranvand, 2024, Nowruzi *et al.* 2024). However, this high metabolic capacity in some strains leads to the production of cyanotoxins-compounds such as microcystins, nodularin, anatoxins, cylindrospermopsin, and other alkaloid or peptide-based toxins, which pose significant hepatotoxic, neurotoxic, and dermatotoxic threats to human health, animal life, and aquatic ecosystems (Mutoti *et al*. 2022).

Toxic blooms of cyanobacteria are a global phenomenon, particularly prevalent in warm, nutrient-rich (eutrophic) environments, leading to sudden increases in cell density and the release of toxins into aquatic systems. Some taxa such as *Microcystis aeruginosa*, *Anabaena*, *Nostoc*, and *Cylindrospermopsis* have frequently been associated with such blooms, resulting in aquatic and terrestrial animal mortality, and even human poisoning events (Bittner *et al*. 2021). Several reports from Golestan Province (Iran), also confirm the occurrence of such toxic blooms in natural water bodies such as Alma-Gol, Aliabad, and Shourmast Wetlands, sometimes linked to animal deaths and human intoxications (Nowruzi *et al.* 2013, Nowruzi *et al*. 2018).

Despite the expansion of taxonomic studies based on morphological features, numerous challenges-such as pronounced morphological variability under culture conditions, structural differences across growth phases, and the influence of environmental factors such as temperature, light, and nutrient composition on colony and cell morphology-have compromised the reliability of classical identification methods. In particular, the accurate and reproducible identification of heterocystous strains like *Nostoc* and *Anabaena* using morphological keys alone is often fraught with error and subject to conflicting interpretations (Komárek 2006).

Accordingly, the necessity of utilizing molecular methods-particularly those based on genomic fingerprinting and the analysis of repetitive DNA sequences-is increasingly recognized. Studies have demonstrated that, the use of molecular markers such as Highly Iterated Palindromes sequences (HIPs), Short Tandemly Repeated Repetitive sequences (STRR), and Enterobacterial Repetitive Intergenic Consensus sequences (ERIC), which are employed in the rep-PCR (repetitive sequence-based polymerase chain reaction) technique, offers a high resolution for distinguishing closely related strains, assessing intraspecific diversity, and analyzing the genetic structure of cyanobacterial populations. These markers are widely distributed and repetitive within prokaryotic genomes and even detect hidden pathogenic strains as the interspecies differences that can be revealed in fingerprinting are not essentially related to the toxin genes of pathogenic related genes (Nowruzi & Hutarova 2023).

In the rep-PCR technique, oligonucleotide primers complementary to the repetitive sequences HIP, ERIC, and STRR are used to amplify the regions flanked by these elements. The resulting products are then separated and analyzed using gel electrophoresis or fluorometric techniques. These DNA banding patterns (DNA fingerprints) yield unique profiles for each strain, which can be employed in similarity analyses, phylogenetic clustering, and the evaluation of both intra- and inter-population genetic diversity. The analysis of these patterns

using computational and bioinformatics tools-such as clustering algorithms, genetic similarity matrices, and phylogenetic trees-can effectively elucidate the evolutionary relationships among isolates and even detect hidden pathogenic strains (Selvakumar & Gopalaswamy 2008).

The widespread presence of repetitive sequences in the genomes of various cyanobacterial species, including *Anabaena* sp. PCC 7120 and *Calothrix*, has facilitated the broad application of rep-PCR, particularly in the taxonomy of heterocystous cyanobacteria. This approach, while maintaining advantages such as rapid processing, high sensitivity, and independence from pure culture isolation, demonstrates significantly greater efficacy than direct sequencing methods like 16S rRNA analysis in differentiating intraspecific strains. This distinction becomes especially important when subtle genetic differences lead to substantial variations in toxin production, pathogenic potential, or environmental responsiveness (Shokraei *et al*. 2019).

Moreover, previous studies conducted in northern Iran, particularly in Golestan Province, have reported high biodiversity and the presence of potentially pathogenic cyanobacterial strains in the aquatic ecosystems of the region. Alma-Gol Wetland, as a natural water reservoir and a source of water for rural communities, is prone to excessive cyanobacterial growth and the occurrence of toxic blooms during warmer seasons. Past reports of mortalities among domestic and wild animals, as well as the identification of toxic strains from the genera *Nostoc*, *Anabaena*, and *Stigonema* in this area, underscore the necessity for a thorough and comprehensive investigation of the cyanobacterial communities inhabiting this wetland (Nowruzi *et al*. 2012). This wetland continues to age due to either natural or human causes, the resulting eutrophication will favor cyanobacterial bloom formation over types of true algae. Therefore, the problem of cyanobacterial bloom formation and subsequent risks to human health are an increasingly important and timely topic. There have been many reports of adverse effects on human health caused by cyanobacteria bloom especially in summer. The majority are of isolated incidents of swimmers developing adverse reactions after bathing in water containing a cyanobacterial bloom. A good example of this is in the allergic reactions shown by two patients accidentally exposed to the cyanobacterial bloom while swimming, who developed hay fever, asthma, and eye irritation. Skin tests showed a positive reaction to the organism. These studies have extended the clinical hazard from simply contact with a bloom, for inhalation of airborne spores or cells. Therefore, rapid and accurate identification of potential toxin producer greatly contributes to strategic planning to prevent the occurrence of toxins in water resources.

The present study is therefore, designed with the objective of molecular identification and genomic fingerprinting of potential toxin producer cyanobacterial strains isolated from Alma-Gol Wetland, utilizing the repetitive molecular markers HIPs, STRR, and ERIC. The application of rep-PCR as a precise, rapid, and sensitive technique-combined with advanced computational analyses-will enable accurate assessments of genetic diversity, molecular phylogeny, and the identification of hazardous strains. In fact, by targeting repetitive sequences in the genome, rep-PCR can be very useful in distinguishing phylogenetically close cyanobacterial genera. This investigation not only represents a fundamental step toward a more refined classification of indigenous Iranian cyanobacteria, but also potentially provides a framework for water health management, the development of biomonitoring strategies, and the prevention of toxic bloom outbreaks in the country's natural water resources.

Materials and Methods

- Sampling and cultivation of water samples

Sampling was conducted in the summer 2024 from the top 10 centimeters of the water surface. During the summer, the surface of Alma-Gol Wetland is consistently green due to the presence of cyanobacterial blooms. Sampling was carried out with three replicates from locations where cyanobacterial blooms were most

concentrated (37°25′03″ N and 54°29′34″ E) (Fig. 1). The samples were immediately transported to the laboratory and inoculated into sterile Z8 medium (Kotai 1972). Liquid, enriched Z8 medium provides a suitable environment for cyanobacteria growth and enrichment. Z8 medium is a valuable tool for culturing and studying these organisms, especially in liquid form, which facilitates inoculation and growth.

The Petri dishes containing the cyanobacterial inoculum were incubated in a growth chamber under continuous fluorescent illumination (40–60 µmol photons m^{-2} s^{-1}) at a temperature of 28–30 ºC for 14 days (Nowruzi & Zakerfirouzabad 2024). In fact, under continuous fluorescent illumination, cyanobacteria utilize their light-harvesting antenna systems, specifically phycobilisomes, to efficiently capture available light.

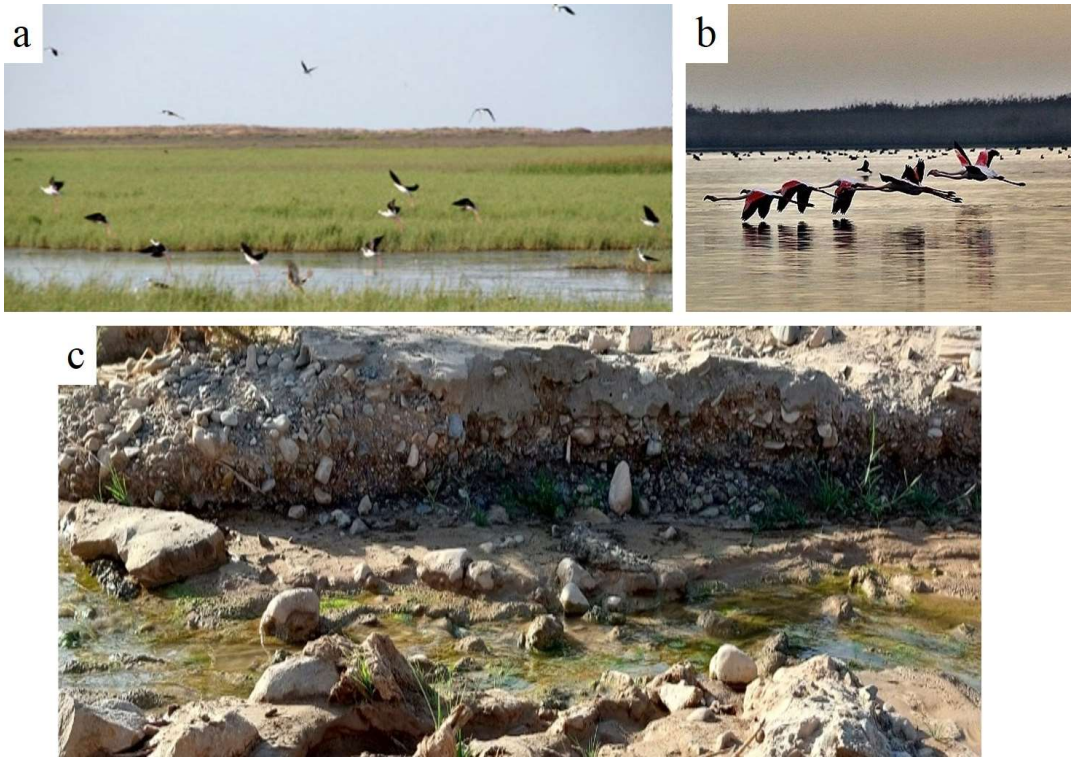

Fig. 1. Alma-Gol Wetland: a. General view and aquatic birds, b. Surrounding landscape, c. Bloom of cyanobacteria strains around the wetland.

- Preparation of solid medium and isolation of strains

To isolate and purify heterocystous cyanobacteria, 10 gr. of agar were added per liter of liquid Z8 medium. Purification was performed three times on solid culture media. After the medium solidified, portions of cyanobacterial colonies exhibiting distinct pigmentation were streaked in a zigzag pattern on the surface. For more precise purification and elimination of microbial contaminants, the motile filament (hormogonium) identification method was employed. This physical trait of cyanobacteria, gliding motility across the surface of solid media, served as a biological criterion to distinguish them from other contaminants. To verify axenic culture status, samples were subsequently cultured in pre-prepared R_2A medium ensuring all other organisms are eliminated to maintain purity. To ensure an axenic culture, purified strains were inoculated point by point onto a plate containing culture medium; the absence of colonies around each inoculation point indicates the purity of the culture (Nowruzi & Lorenzi 2024).

- Morphological identification

A morphological observation of the culture utilized an Olympus CX31RTS5 (Olympus, Tokyo, Japan) stereoscope equipped with a QImaging GO-3 digital camera (Teledyne QIMAGING, Surrey, Canada) and Olympus BX43 equipped with manufactured Sc50 digital

camera (Olympus, Tokyo, Japan). A preliminary identification was done using the keys by Desikachary (1959) with the revisions of Komárek et al. (2013).

- Genomic DNA extraction

Genomic DNA was extracted manually using the phenol-chloroform method (Baptista *et al*. 2021). DNA concentration was measured using a NanoDrop spectrophotometer, and absorbance was recorded at wavelengths of 260 and 280 nm. The concentration was expressed in ng/µL. To assess DNA quality, samples were electrophoresed in 1% agarose gels (SeaPlaque® GTG®, Cambrex) prepared in 1X TAE buffer, diluted from a 50X TAE stock solution. DNA bands were visualized under UV illumination using a Gel Doc XR transilluminator (Bio-Rad) and analyzed with QUANTITY ONE® software Ver. 4.6.7 (Baptista *et al*. 2021).

- Genomic fingerprinting analysis

To analyze the genetic structure of the isolates, rep-PCR was performed using three types of repetitive DNA markers: HIP, STRR, and ERIC. The primers used are listed in table 1. PCR reactions were carried out in a final volume of 25 µL, containing 12.5 µL of master mix, 0.5 µL of each primer, 2 µL of template DNA, and 9.5 µL of PCR-grade water (Nowruzi & Hutarova 2023).

- Primers and PCR program for amplification of HIP, ERIC and STRR repetitive sequences

Thermal cycling conditions varied depending on the primer set. For ERIC-PCR reactions, initial denaturation was conducted at 95 ºC for 7 min., followed by 30 cycles of denaturation at 94 ºC for 1 min., annealing at 52 ºC for 1 min., and extension at 65 ºC for 8 min.. A final extension step was performed at 65 ºC for 16 min. (Nowruzi & Fahimi 2022). For HIP-PCR reactions using HIP-TG, HIP-GC, and HIP-CA primers, initial denaturation was at 95 ºC for 5 min., followed by 30 cycles of denaturation at 95 ºC for 30 sec., annealing at 30 ºC for 30 sec., and extension at 72 ºC for 60 sec.. Final extension was carried out at 72 ºC for 5 min. (Nowruzi & Fahimi 2022). STRR-PCR reactions began with initial denaturation at 95 ºC for 6 min., followed by 30 cycles of denaturation at 94 ºC for 1 min., annealing at 56 ºC for 1 min., and extension at 65 ºC for 5 min.. The final extension step was performed at 65 ºC for 16 min. (Singh *et al*. 2014). Following PCR amplification, the products were electrophoresed alongside appropriate DNA size markers. Band size ranges were carefully assessed, and size intervals (e.g., 300–400, 400–500 bp, etc.) were defined for each marker and strain. The presence or absence of bands in each interval was recorded as binary data (1/0). Genomic fingerprinting analysis of highly repetitive palindromic sequences was conducted using Biodiversity Pro-software (Singh *et al*. 2014, Shokraei *et al*. 2019).

Table 1. List of highly repetitive palindromic primers used for HIP, STRR and ERIC-PCR

Target gene	Sequence 5´ 3´	Reference
ERIC1A	ATGTAAGCTCCTGGGGATTCAC	De Bruijn (1992)
ERIC1B	AAGTAAGTGACTGGGGTGAGCG	De Bruijn (1992)
STRR1A	CCARTCCCCARTCCCC	Rasmussen & Svenning (1998)
HIP-TG	GCGATCGCTG	Smith *et al*. (1998)
HIP-GC	GCGATCGCGC	Smith *et al*. (1998)
HIP-CA	GCGATCGCCA	Smith *et al*. (1998)

- PCR amplification of *mcy* genes for detection of toxigenic cyanobacteria

Amplification of the *mcyG*, *mcyD* and *mcyE* genes was performed using specific primers to identify potentially toxic cyanobacterial strains (Table 2). Each PCR reaction was conducted in a final volume of 25 µL, containing 12.5 µL of 2 × Master Mix, 1 µL of forward primer, 1 µL of reverse primer, 2 µL of template DNA, and 8.5 µL of PCR-grade water.

PCR reactions targeting *mcyD*, *mcyG* and *mcyE* genes were carried out under thermal cycling conditions described by Nowruzi & Lorenzi (2021): an initial denaturation at 95 ºC for 5 min., followed by 30 cycles of denaturation at 95 ºC for 30 sec., annealing at 53 ºC for 30 sec., and extension at 72 ºC for 1 min., with a final extension at 72 ºC for 5 min. (Nowruzi *et al*. 2021).

Table 2. List of primers used for amplification of *mcy* genes

Target gene	Sequence 5´ 3´	Amplicon size	Reference
mcyGF *mcyGR*	GAAATTGGTGCGGGAACTGGAG TTTGAGCAACAATGATACTTTGCT	247 bp	Fewer *et al*. (2007)
mcyDF *mcyDR*	GATCCGATTGAATTAGAAAG GTATTCCCCAAGATTGCC	818 bp	Rantala *et al*. (2006)
mcyEF *mcyER*	GAAATTTGTGTAGAAGGTGC AATTCTAAAGCCCAAAGACG	812 bp	

- Identification based on 16S rRNA and ITS sequences

Following the identification of the five pathogenic strain carrying the *mcy* gene, for molecular identification, the 16S rRNA and ITS gene regions were amplified. PCR reactions were prepared in 50 µL volumes in three replicates per sample, one positive control, and one negative control. Reactions were conducted using an iCycler thermal cycler

(Bio-Rad) (Nowruzi & Shalygin 2021).

ITS is a suitable marker for investigating intraspecific diversity in cyanobacteria. The ITS region exhibits significantly higher variability compared to the 16S rRNA gene (Nowruzi & Shalygin 2021). The primers used for PCR are listed in table 3. PCR is comprised of four cycles. The first cycle was the initial denaturation step at 94 ºC for 5 min.. The second cycle consisted of three steps: the first step was denaturation at 94 ºC for 30 sec.; the second step was annealing, during which primers bind to the template DNA single strands, performed at 56 ºC for 30 sec.; and the third step was extension at 72 ºC for 2 min.. The third cycle, termed final extension, conducted at 72 ºC for 15 min.. The fourth cycle, designated the final hold, maintained at 4 ºC.

Table 3. Primers used in the PCR reactions (Nowruzi & Shalygin 2021)

Target gene		Sequence 5´ 3´	Reference
16S rRNA	27F1	AGAGTTTGATCCTGGCTCAG (8-27)	Neilan *et al*. (1997)
	23S30Ra	CTTCGCCTCTGTGTGCCTAGGT (30-52)	Lepère *et al*. (2000)
ITS	ITS16CF	CCATGGAAGYTGGTCAYG (1411-1428) (16S)	Iteman *et al*. (2000)
	ITS23CR	CCTCTGTGTGCCTAGGTATCC (26-46) (23S)	Iteman *et al*. (2000)

- Secondary structure analysis of the ITS region using the Mfold Program

Secondary structure analysis of the ITS region was performed using the Mfold web server. The "RNA Folding Form" option was selected, and the target sequence was submitted. In the "STRUCTURE DRAW MODE" section, the 'Untangle with loop fix' option was selected, followed by the "fold RNA" command. The secondary structures of the D1-D1′ and Box-B regions were visualized, and the number of nucleotides, their spacing, and the number of loops were analyzed (Nowruzi *et al*. 2023).

- Phylogenetic tree construction

Upon confirming the accuracy of the forward and reverse sequences, pairwise alignment was performed using the BioEdit software Ver. 7 to generate consensus sequences. Subsequently, BLASTN searches were conducted for the 16S rRNA and ITS genes (1250 bp), and BLASTX was used for the *mcyD* (540 bp) gene. Following retrieval of similar sequences, multiple sequence alignment was conducted using MAFFT Ver. 7. In this method, several parameters selected to influence the accuracy, speed, and specific type of alignment produced. These include options for progressive, iterative refinement, and structural alignment methods.

Phylogenetic trees were constructed using the IQ-TREE online program based on the Maximum Likelihood method after model selection (16S rRNA: TVM+G4; *mcy*: TIM2+F). Different models were used as suggested (BIC criterion) after employing model test implemented in IQ-tree. Tree robustness was estimated with bootstrap percentages using 100 standard bootstrap and 10,000 ultrafast bootstrap to evaluate branch supports (Guajardo-Leiva *et al*. 2018). Final modifications were made using the FigTree software Ver. 1.4.4. (Nowruzi & Soares 2021).

Results

- Culturing results of water samples in Z8 medium

Different stages of culturing, isolation, and purification of water samples from Alma-Gol wetland are shown in figures 2–3. Among the cultured water samples, five colonies exhibiting different colors and morphologies were observed. After several rounds of sub-culturing on solid media, pure colonies were obtained.

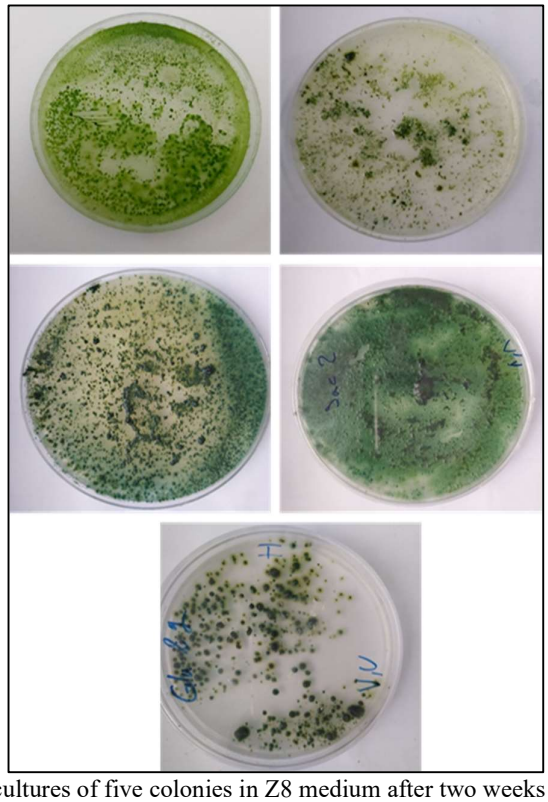

Fig. 2. Final cultures of five colonies in Z8 medium after two weeks of incubation.

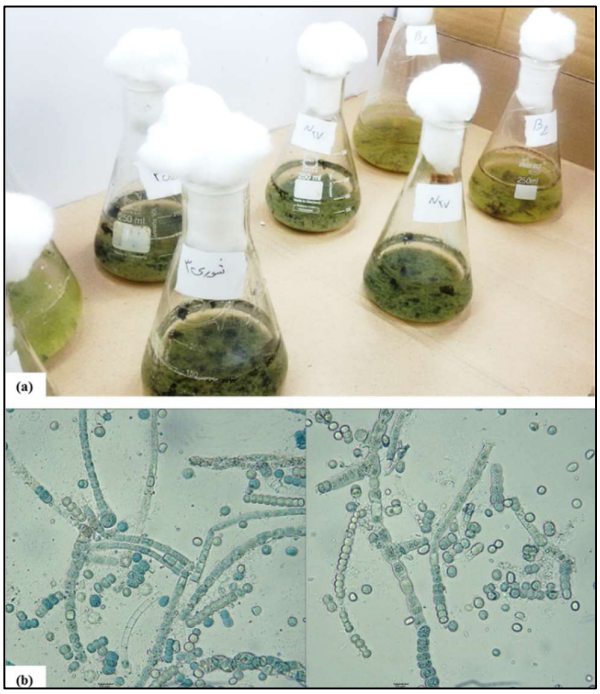

Fig. 3. a. Cultured purified colonies in liquid medium, b. Purification process using hormogonia on agar medium (magnification: 100X).

- Taxonomic classification of studied strains

Morphological studies identified five distinct strains (Fig. 4). The *Nostoc* sp. 9, *Aliinostoc* sp. 1, and *Desmonostoc* sp. 10 belong to Nostocaceae (cyanobacteria), whereas *Calothrix* sp. 7 belongs to Calotrichaceae, and *Neowestiellopsis* sp. 2 to Hapalosiphonaceae. The Nostocaceae that forms filament-shaped colonies enclosed in mucus or a gelatinous sheath. Calotrichaceae, a tapering heterocytous cyanobacteria, found in freshwater and terrestrial habitats, whereas Hapalosiphonaceae consists of filamentous and multiseriate cyanobacteria.

Neowestiellopsis sp. 2 is characterized by true branching observed along the trichome. *Desmonostoc* sp. 10 is recognized by vegetative cells, intercalary apical heterocytes (usually spherical) located at the terminal ends of hormogonia. Moreover, separated hormogonia are observed throughout. *Aliinostoc* sp. 1, identified by the presence of rectangular heterocytes within the filament and spherical heterocytes at the end of the trichome. *Calothrix* sp. 7 distinguished by the formation of numerous hormogonia along the trichome, which serve a reproductive function. Additionally, it exhibits larger vegetative cells at the base of the trichome, with the cells gradually tapering toward the terminal end, a key feature that characterize this genus. *Nostoc* sp. 9, characterized by spherical heterocytes and rectangular vegetative cells along the trichome.

- DNA concentration determination results

NanoDrop analysis indicated that, the DNA purity of all samples fell within the standard range (Table 4).

- Results of genomic fingerprinting analysis based on highly repetitive primers

The electrophoresis gels resulting from amplification of STRR bands in the five tested colonies are shown in figure 5 a. Analysis of the STRR cluster results revealed that, *Neowestiellopsis* sp. 2 and *Calothrix* sp. 7 grouped into a single cluster (Fig. 6). Based on the original similarity matrix and the matrix obtained by the dendrogram, the cophenetic correlation was 70%. *Desmonostoc* sp. 10 formed the most distant clade, exhibiting the lowest genetic relatedness to the other isolates. Likewise, the electrophoresis gels from HIP-TG band amplification in the five tested colonies are shown in figure 5 b. The HIP-TG dendrogram demonstrated that, *Neowestiellopsis* sp. 2 formed the most distant clade and

exhibited the lowest relatedness to the other isolates (Fig. 6 b). *Calothrix* sp. 7 appeared as a separate branch outside the Nostocaceae clade (Table 5).

- Results of band count from palindromic sequence fingerprinting and amplification

Analysis of the amplified palindromic sequences indicated that, the highest number of amplified bands was obtained using ERIC1A primers, while the lowest was observed with HIP-CA. The highest number of amplified bands indicates that, this part of genome plays a crucial role in genome structure, function, and evolution. The strains producing the greatest number of amplified bands were *Aliinostoc* sp. 1 and *Calothrix* sp. 7 (Fig. 7, Table 6).

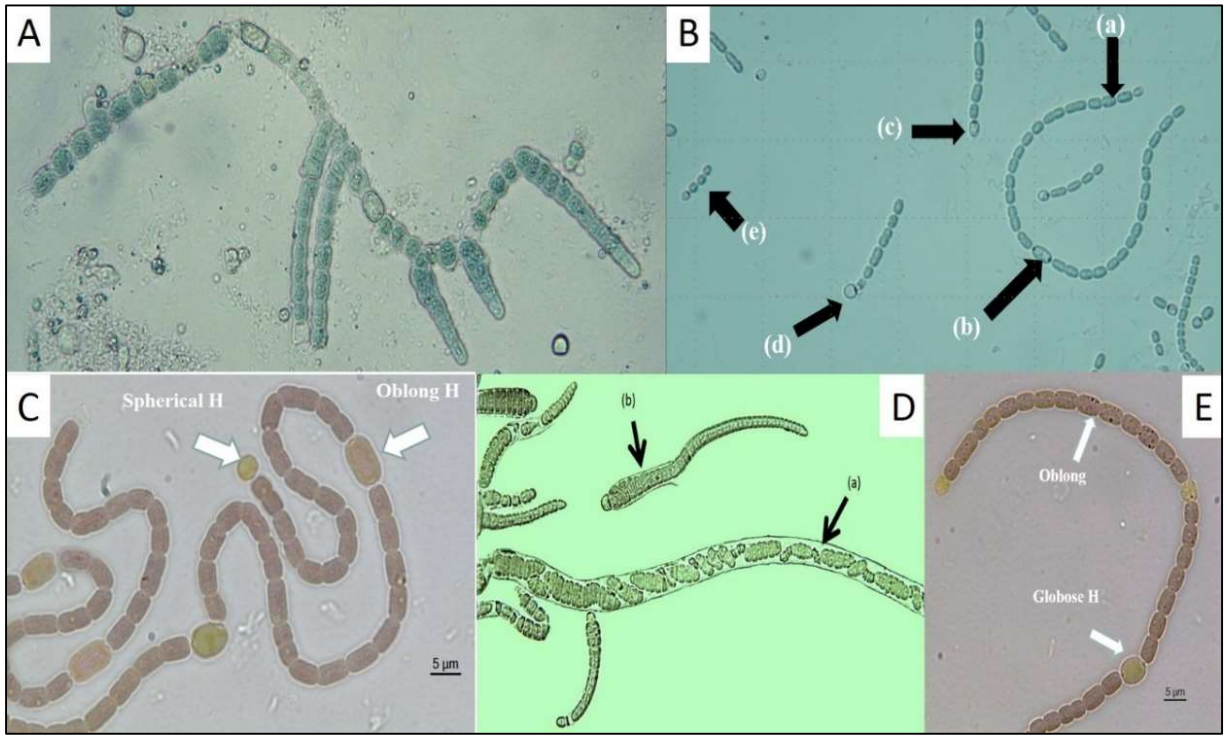

Fig 4. Purified cyanobacterial strains: A. *Neowestiellopsis* sp. 2, B. *Desmonostoc* sp. 10 [a. Vegetative cells, b. Intercalary heterocytes, c. Apical heterocytes, d. Spherical heterocytes located at the terminal end of hormogonia, e. Separated hormogonia], C. *Aliinostoc* sp. 1, D. *Calothrix* sp. 7 [a. Hormogonia, b. Larger vegetative cells], E. *Nostoc* sp. 9.

Table 4. DNA concentration and purity measured using NanoDrop (ng/µL)

Colony	Concentration (ng/µl)	A260 (AU)	A280 (AU)	A260/A280 ratio	A260/A230 ratio
1	258.31	5.166	2.739	1.89	2.14
2	46.29	0.92	0.49	1.89	2.2
3	31.52	0.89	2.03	1.81	2.1
4	141.81	2.836	1.508	1.88	2.09
5	21.05	0.421	0.224	1.88	2

Table 5. Original similarity matrix and the matrix obtained by the dendrogram and the cophenetic correlation

Palindromic primer	Similarity
ERIC1A	*Nostoc* sp. 9 and *Aliinostoc* sp. 1 were grouped in a clade with 75% similarity. *Desmonostoc* sp. 10 and *Calothrix* sp. 7 were placed in separate branches, each with 75% similarity, relative to the two aforementioned strains. *Neowestiellopsis* sp. 2, with 55% similarity, was placed in a distinct and genetically distant branch.
ERIC1B	*Nostoc* sp. 9 and *Aliinostoc* sp. 1 grouped into a clade with 90% similarity. *Desmonostoc* sp. 10, with 70% similarity, appeared in a separate branch. *Calothrix* sp. 7 and *Neowestiellopsis* sp. 2 were each located in individual branches with 50% similarity, showing considerable genetic distance from the previous three strains.
HIP CA	*Desmonostoc* sp. 10 and *Nostoc* sp. 9 clustered together with 60% similarity. However, *Aliinostoc* sp. 1 was placed in a separate branch with 50% similarity to the aforementioned two strains. *Calothrix* sp. 7 and *Neowestiellopsis* sp. 2 formed a cluster with 60% similarity.
HIP AT	*Aliinostoc* sp. 1 and *Nostoc* sp. 9 clustered together with 85% similarity. *Desmonostoc* sp. 10 and *Calothrix* sp. 7 each appeared in separate branches with 65% similarity, while *Neowestiellopsis* sp. 2 was positioned in a distinct and most distant clade.
HIP TG	*Aliinostoc* sp. 1, *Nostoc* sp. 9, and *Desmonostoc* sp. 10 grouped into a cluster with 70% similarity.
HIP GC	*Nostoc* sp. 9 and *Aliinostoc* sp. 1 grouped into a clade with 100% similarity. *Desmonostoc* sp. 10, with 75% similarity, was placed in a separate branch relative to these two strains. *Calothrix* sp. 7 and *Neowestiellopsis* sp. 2 clustered together with 60% similarity but were positioned at a considerable genetic distance from the former three strains.
STRR	*Aliinostoc* sp. 1 and *Nostoc* sp. 9 were classified within the same clade with 60% similarity.

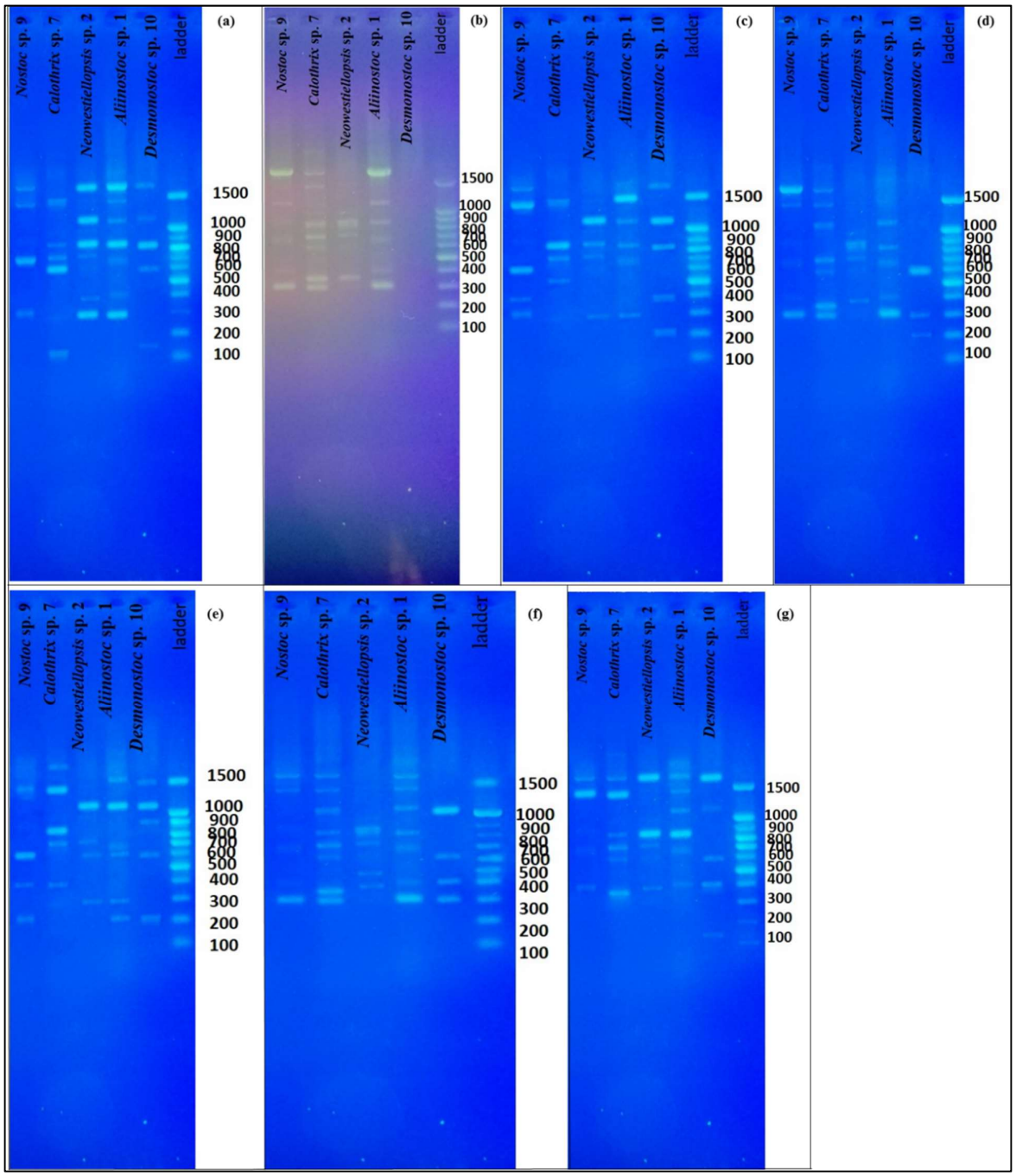

Fig. 5. Electrophoresis gels of PCR products for the five tested colonies using primers: a. STRR, b. HIP-TG, c. HIP-AT, d. HIP-CA, e. HIP-GC, f. ERIC A, g. ERIC B.

- Results of band count from palindromic sequence fingerprinting and amplification

Analysis of the amplified palindromic sequences indicated that, the highest number of amplified bands was obtained using ERIC1A primers, while the lowest was observed with HIP-CA. The highest number of amplified bands indicates that, this part of genome plays a crucial role in genome structure, function, and evolution. The strains producing the greatest number of amplified bands were *Aliinostoc* sp. 1 and *Calothrix* sp. 7 (Fig. 7, Table 6).

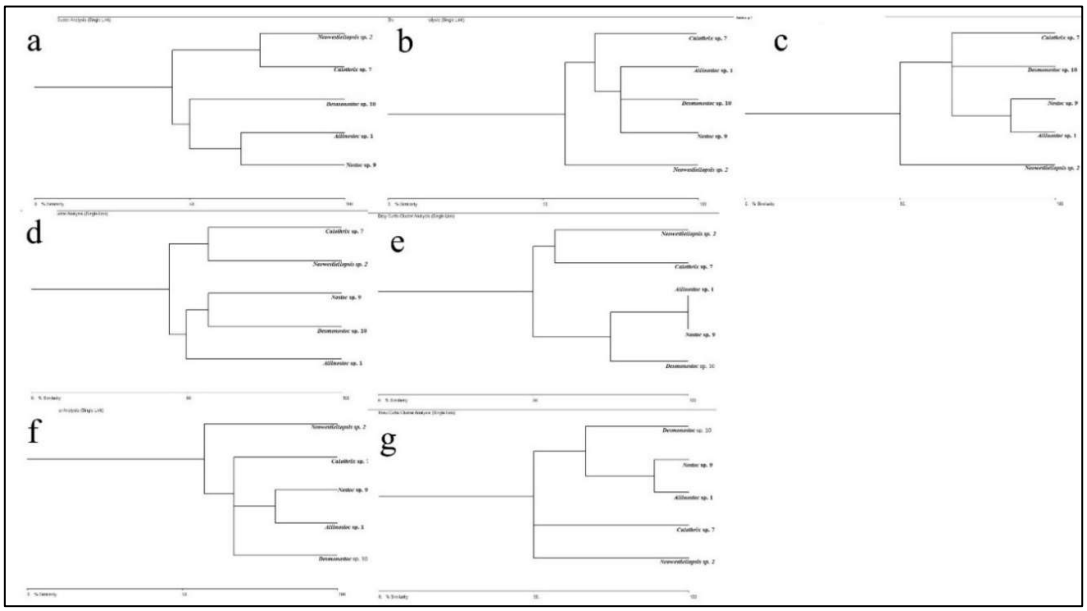

Fig. 6. Dendrogram from cluster analysis of STRR, HIP and ERIC markers in five cyanobacterial isolates: a. STRR dendrogram, b. HIP-TG dendrogram, c. HIP-AT dendrogram, d. HIP-CA dendrogram, e. HIP-GC dendrogram, f. ERIC A dendrogram, g. ERIC B dendrogram.

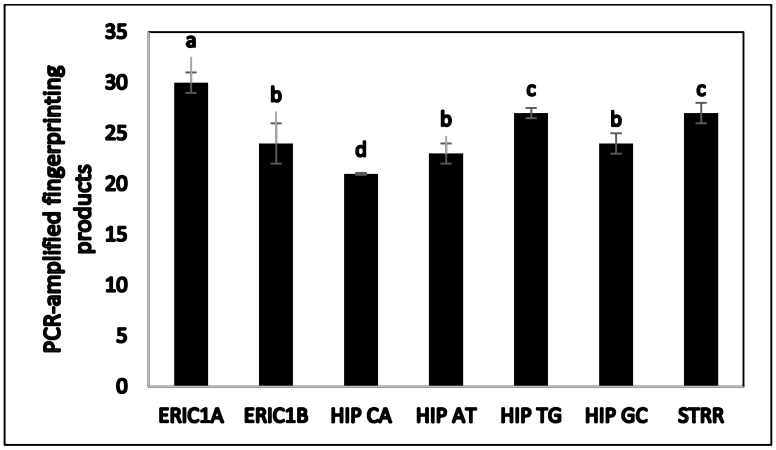

Fig. 7. Results of one-way analysis of variance (ANOVA) of PCR-amplified fingerprinting products for the studied cyanobacterial strains. Little letters means there are not significantly different between groups ($P<0.05$).

Table 6. Number of PCR-amplified fingerprinting products for the studied cyanobacterial strains

Palindromic primer	*Aliinostoc* sp. 1	*Desmonostoc* sp. 10	*Nostoc* sp. 9	*Calothrix* sp. 7	*Neowestiellopsis* sp. 2	Total
ERIC1A	8	4	6	8	4	30
ERIC1B	6	5	3	6	4	24
HIP CA	5	3	3	7	3	21
HIP AT	5	5	5	4	4	23
HIP TG	6	3	6	8	4	27
HIP GC	6	5	4	5	4	24
STRR	7	5	4	5	6	27

- Results of phylogenetic tree construction based on the *mcy* gene

Amplification of the *mcyG*, *mcyD*, and *mcyE* genes was performed using specific primers to identify potentially toxigenic strains. Among the amplified genes, only the *mcyD* gene, approximately 818 bp in size, was successfully detected. The resulting phylogenetic tree, constructed based on BLAST analysis of the shared sequence, is illustrated in figure 8. As shown here, the detected gene in the studied strain belongs to the Hapalosiphonaceae and clusters with other members of this family in a highly related clade. Notably, the *mcyD* containing strain clustered with *Fischerella* sp. LSKH with a bootstrap value of 98.3%.

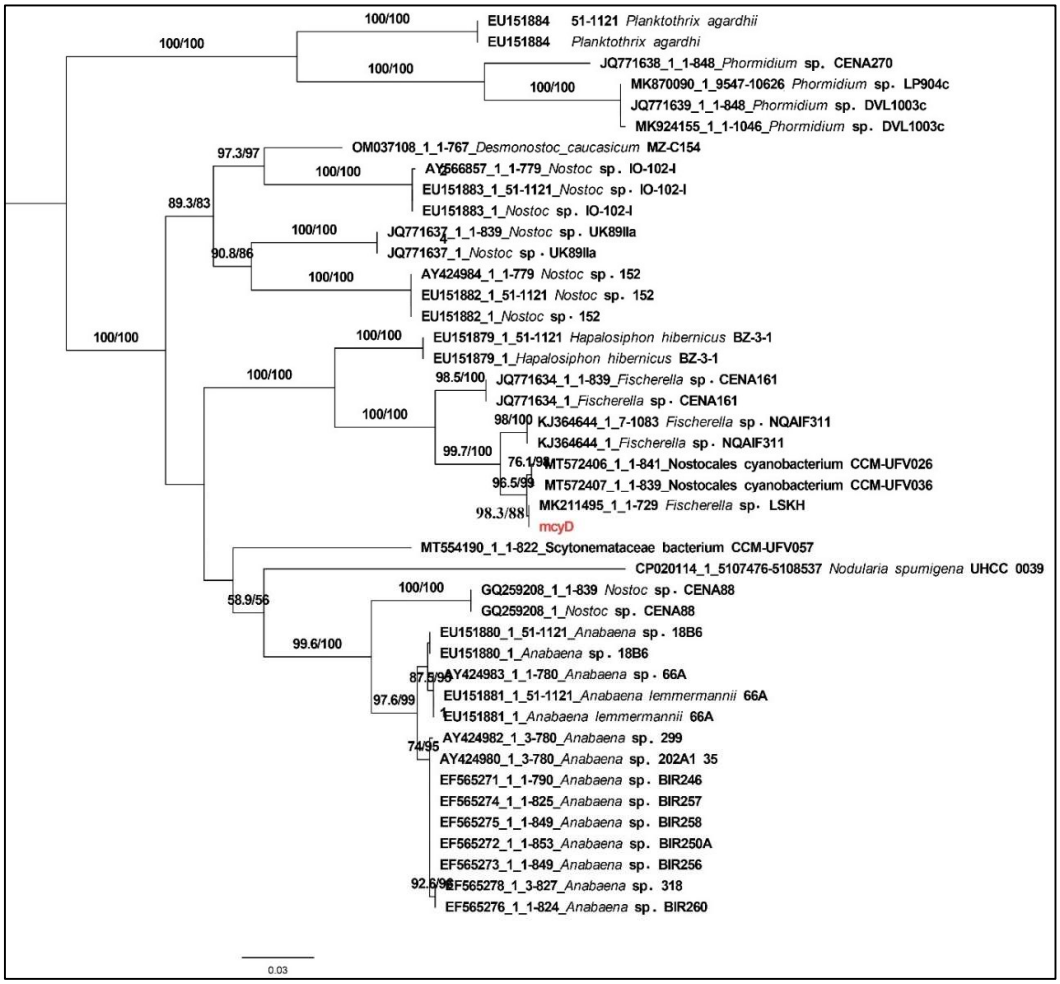

Fig. 8. Phylogenetic tree based on the *mcyD* gene. The resulting scale of 0.03 indicates the number of nucleotide substitutions per site.

- Results of electrophoresis of the 16S rRNA gene PCR product

Following the identification of the pathogenic strain containing the *mcyD* gene, molecular identification of the strain was conducted through amplification of the ITS and 16S rRNA genes. The phylogenetic tree constructed based on the 16S rRNA gene showed a correlation with the morphological identification of the five studied strains. All five strains clustered separately within distinct clades corresponding to different genera in their respective families. All clades and associated genera are clearly indicated in figure 9, along with the family names. Furthermore, a strong correlation was observed between the tree generated from the 16S rRNA gene and the one derived from the *mcyD* gene. The target strain clustered with other members of the Hapalosiphonaceae within a single clade supported by a high bootstrap value of 93.5%.

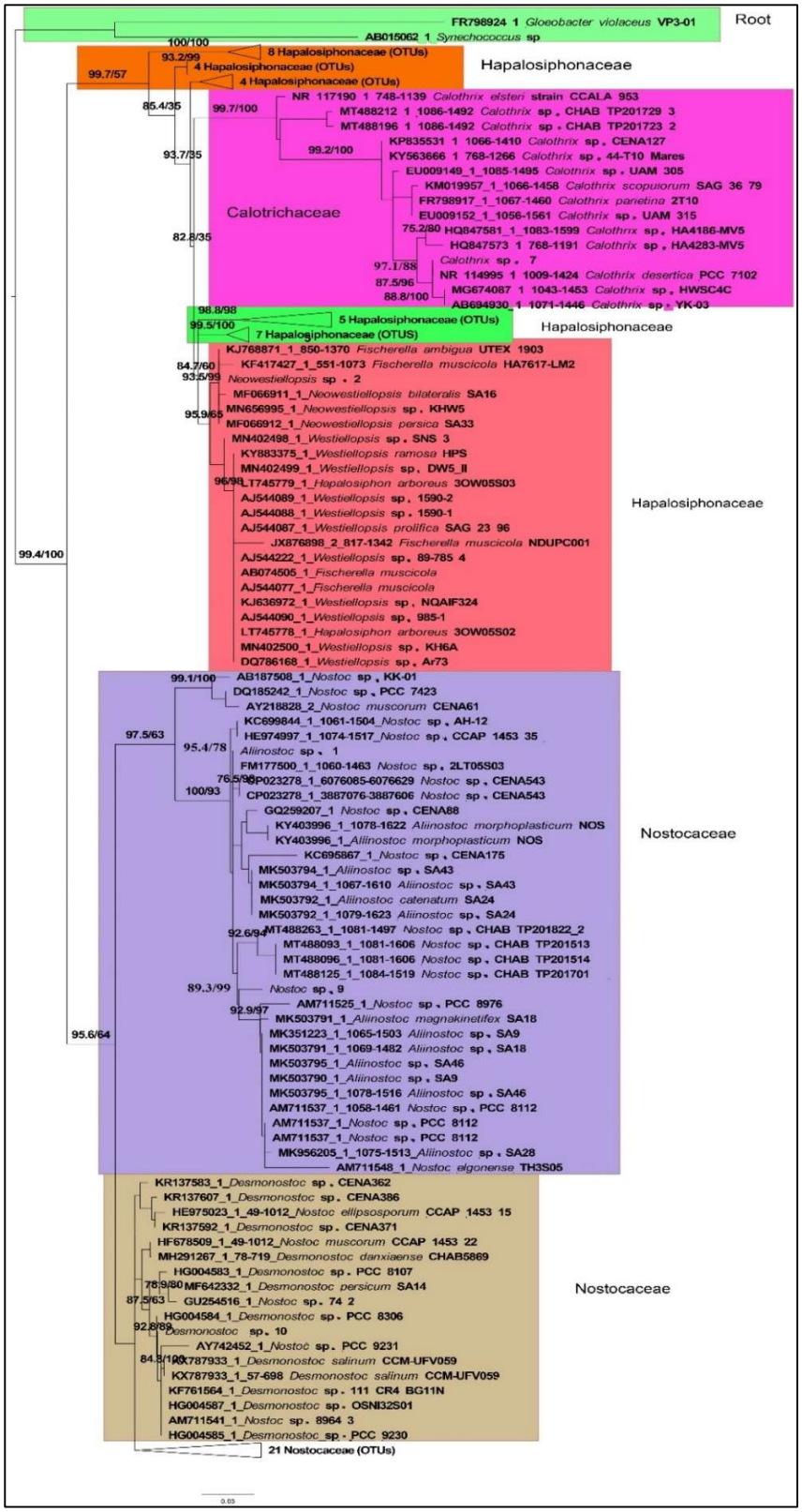

Fig. 9. Phylogenetic tree constructed based on the 16S rRNA gene. The resulting scale of 0.03 indicates the number of nucleotide substitutions per site.

- Secondary structure analysis of the ITS region using the Mfold Program

The ITS region structure was analyzed to identify the D1-D1′ helix, D2, D3, *trnI* (Ile) gene, *trnA* (Ala) gene, BOX B, and BOX A. Comparative analysis of the ITS region lengths between the target strain and other phylogenetically related strains from the phylogenetic tree revealed that, the lengths of the D1-D1′ helix and BOX B regions differed from those of the other strains. Additionally, secondary structure predictions of the D1-D1′ helix and BOX B regions produced distinct structural patterns (Figs 10–12, Tabs 7–8).

Table 7. Comparison of ITS region lengths between the target strain and other phylogenetically related strains from the phylogenetic tree

Studied strain with related sequence/ accession number	D1-D1′ helix (bp)	D2 with spacer (bp)	$tRNA^{Ile}$ gene (bp)	$tRNA^{Ala}$ gene (bp)	BOX B (bp)	Post-BOX B spacer (bp)	BOX A (bp)
Neowestiellopsis sp. 2	72	19	74	73	30	17	11
>KF417427.1 *Fischerella muscicola* HA7617-LM2	71	19	74	73	29	17	11
>KT715746.1 *Fischerella* sp. CY9	63	19	-	-	40	17	28
>MN656995.1 *Neowestiellopsis* sp. KHW5	71	19	73	73	29	23	13
>DQ786171.1 *Fischerella* sp. MV11	107	19	74	73	29	17	11
>DQ786172.1 *Fischerella* sp. RV14	97	19	-	-	31	17	11
>DQ786170.1 *Fischerella* sp. MV11	107	19	-	-	31	18	11
>DQ786173.1 *Fischerella* sp. RV14	107	19	74	74	29	17	11
>KT715745.1 *Fischerella* sp. CY2	63	19	-	-	31	17	11

Table 8. Comparative analysis of ITS secondary structures (D1-D1′ helix and BOX-B) between the target strain and other phylogenetically related strains

Studied strain with related sequence/ accession number	D1-D1′ helix				BOX-B	
	Terminal bilateral bulge (A)	Bilateral bulge (B)	Unilateral bulge (C)	Basal bilateral bulge (D)	Terminal bilateral bulge (A)	Bilateral bulge (B)
	Nucleotide count	Loop count	Loop count		Nucleotide count	
Neowestiellopsis sp. 2	8	1	3	10	13	7
>KF417427.1 *Fischerella muscicola* HA7617-LM2	8	2	2	10	12	7
>KT715746.1 *Fischerella* sp. CY9	9	1	1	6	6	16
>MN656995.1 *Neowestiellopsis* sp. KHW5	9	1	1	6	8	15
>DQ786171.1 *Fischerella* sp. MV11	5	2	1	22	6	15
>DQ786172.1 *Fischerella* sp. RV14	5	2	1	22	6	15
>DQ786170.1 *Fischerella* sp. MV11	5	3	2	6	6	-
>DQ786173.1 *Fischerella* sp. RV14	5	3	2	6	6	-
>KT715745.1 *Fischerella* sp. CY2	8	2	2	10	-	11

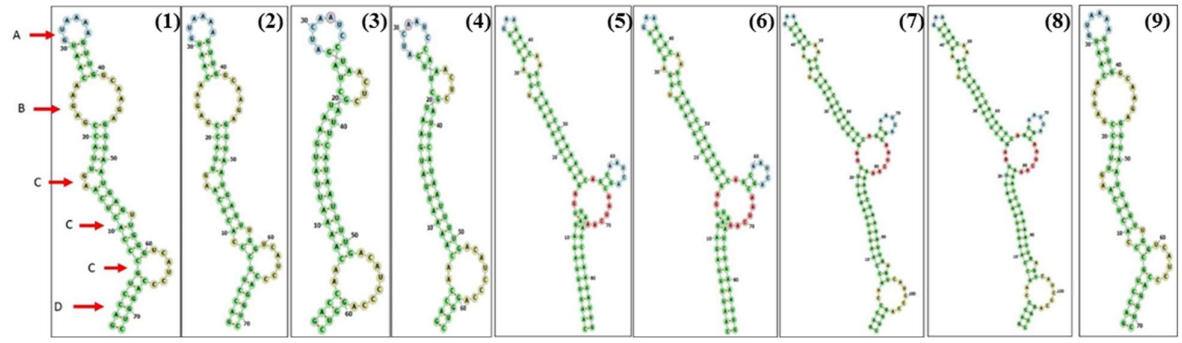

Fig. 10. Identification of various structural regions in the D1-D1′ helix: A. Terminal bilateral bulge, B. Bilateral bulge, C. Unilateral bulge, D. Basal bilateral bulge [(1) *Neowestiellopsis* sp. 2, (2) KF417427, (3) KT715746.1, (4) KT715745.1, (5) DQ786172.1, (6) DQ786170.1, (7) DQ786173.1, (8) DQ786171.1, (9) MN656995.1].

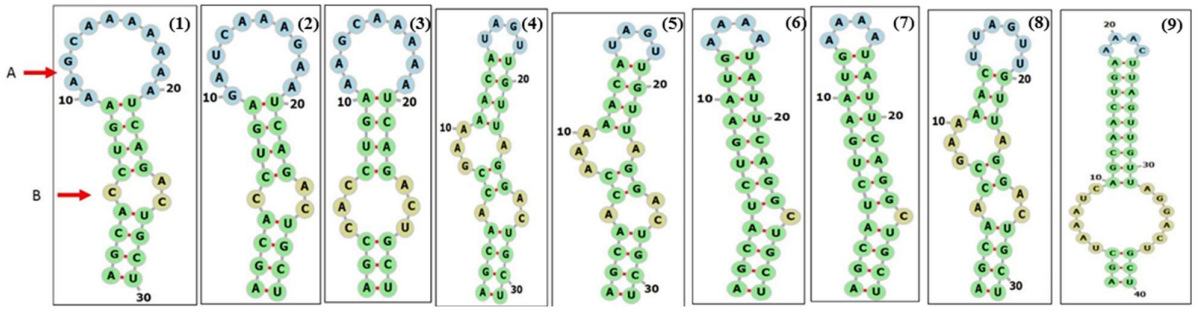

Fig. 11. Identification of various structural regions in the BOX-B helix: A. Terminal bilateral bulge; B. Bilateral bulge [(1) *Neowestiellopsis* sp. 2, (2) KF417427, (3) KT715746.1, (4) KT715745.1, (5) DQ786172.1, (6) DQ786170.1, (7) DQ786173.1, (8) DQ786171.1, (9) MN656995.1].

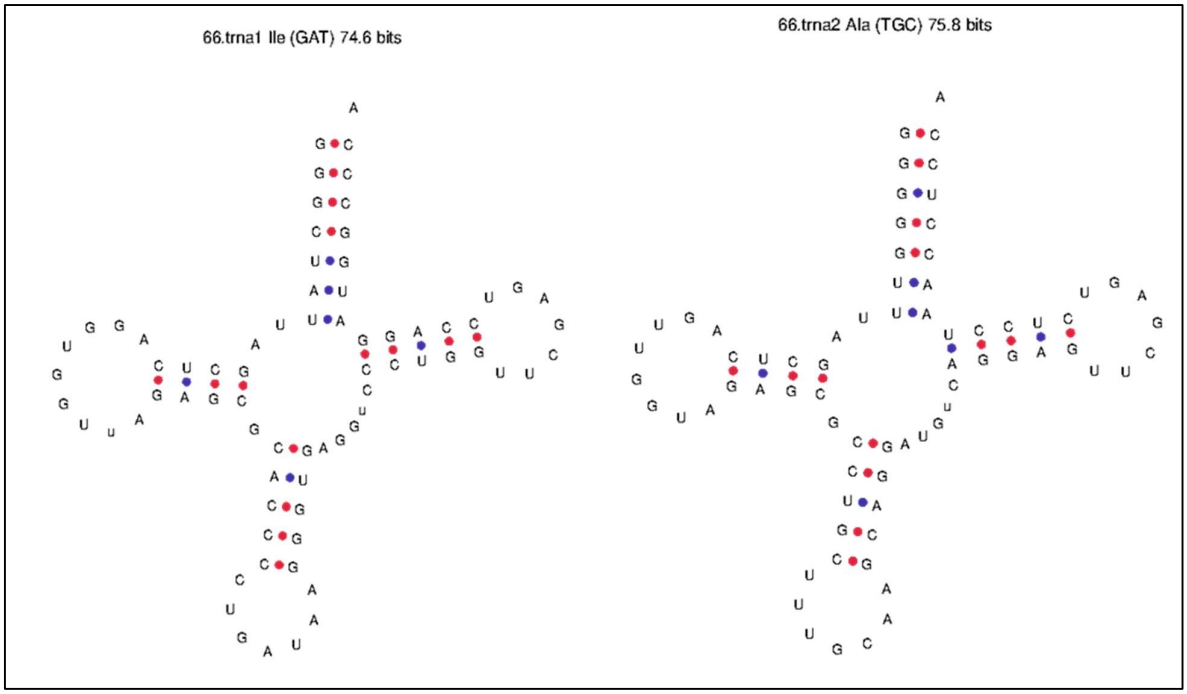

Fig. 12. Predicted secondary structures of tRNA genes: *trnI* (isoleucine, anticodon GAT) on the left, and *trnA* (alanine, anticodon TGC) on the right, identified in the ITS region.

Discussion

The identification of various cyanobacterial species has traditionally relied on evolutionary and morphological characteristics. However, these features are not always reliable, and accurate identification of cyanobacteria using such methods remains challenging due to the high plasticity of phenotypic traits. Features such as heterocyst morphology, trichome branching patterns, and colony architecture are influenced by environmental conditions and cultivation methods (Becerra-Absalón *et al*. 2013). In this study, a polyphasic approach incorporating morphological assessments, 16S rRNA and ITS gene sequencing, genomic fingerprinting using HIP, STRR, and ERIC markers, and bioinformatics analyses enabled the precise identification of five heterocytous cyanobacterial strains isolated from Alma-Gol Wetland. These included three strains from the Nostocaceae, one from Calotrichaceae, and a toxic strain belonging to the Hapalosiphonaceae. These findings are consistent with previous studies and highlight the considerable genetic diversity of cyanobacteria in northern Iran.

One of the key findings of this study was the identification of *Neowestiellopsis* sp. 2 as the only strain harboring the *mcyD* gene. Sequencing and phylogenetic analysis of this gene confirmed its affiliation with the Hapalosiphonaceae. This strain exhibited potential toxin production and a unique banding pattern in rep-PCR profiling.

A similar study conducted by Tavakoli *et al.* (2021) on Latian Lake in Tehran also demonstrated significant genetic and toxigenic diversity among freshwater cyanobacteria in Iran (Tavakoli *et al*. 2021). In that study, nine cyanobacterial species were identified, belonging to the Synechococcales, Oscillatoriales, and Nostocales. Furthermore, microcystin production was reported in *Phormidium* sp. with the detection of the *mcyE* gene, cylindrospermopsin production in *Cyanobium* and *Limnothrix* strains, and the presence of anatoxin in genera such as *Calothrix*. These findings reinforce the potential for toxin production in native Iranian strains and underscore the need for further detailed investigations in various regions, including Alma-Gol Wetland.

Analyses based on photosynthetic pigments, isozyme variations, or cultivation of differentiated cells may also be misleading, as gene expression in cyanobacteria is variable. Therefore, the application of molecular tools is essential to overcome such limitations. In fact, the integration of phenotypic traits with molecular markers represents a more robust method for understanding molecular affinities, cyanobacterial systematics, and the composition of natural cyanobacterial communities (Selvakumar & Gopalaswamy 2008).

Today, genomic fingerprinting using primers such as ERIC, STRR1a, HIP-GC, HIP-CA, HIP-AT, and HIP-TG is widely employed for intra-species comparisons among cyanobacteria (Hulton *et al*. 1991, Wilson *et al*. 2000, Orcutt *et al*. 2002, Zheng *et al*. 2002, Neilan *et al*. 2003, Chonudomkul *et al*. 2004, Wilson *et al*. 2005, Valerio *et al*. 2009, Akoijam & Singh 2011).

In a study performed by Cai *et al.* (2020), two cyanobacterial strains morphologically similar to *Nostoc* species were isolated from rock surfaces in China and identified. Although these strains appeared indistinguishable from typical *Nostoc* species in both field and cultured samples, phylogenetic analyses based on the 16S rRNA gene and the secondary structure of the ITS region (including domains D1-D1', Box-B, and the V3 helix) revealed significant divergence from *Nostoc sensu stricto.* These findings led to the proposal of a new genus and species i.e., *Violetonostoc minutum* (Cai *et al*. 2020). Like the present study, this work underscores the importance of polyphasic approaches and the integration of morphological and molecular data in the accurate classification of cyanobacteria.

A survey conducted by Rouhiainen *et al.* (1995) using STRR sequences, successfully identified toxin-producing cyanobacterial strains. In another study conducted by Valério *et al.* (2009), STRR in combination with other molecular targets such as 16S rRNA, *mcy* and ERIC was employed to identify and trace freshwater cyanobacterial strains.

Based on a different study made by Nowruzi *et al.* (2012), the identification and toxic potential of a cyanobacterial strain from the genus *Nostoc*, isolated from Iranian rice paddies, were also investigated. This study employed molecular analysis of the *nosF* gene in strain ASN-M and LC-MS to identify three classes of peptide compounds: anatoxin, cryptophycins, and nostocyclopeptides. Although common toxins such as anatoxin-a and microcystins were not detected, the results suggest a possible role of these compounds in the observed animal mortalities near the rice fields. This work represents the first documented report of cyanobacteria-associated toxicity in animals in Iran (Nowruzi *et al*. 2012).

Another study conducted by Shokraei *et al.* (2019) was also aligned with the objectives of the present research. In this study, seven cyanobacterial strains were isolated from various regions in Iran, including agricultural areas, saline waters, and dry limestone substrates. The results indicated no significant morphological differences among these strains. Therefore, to achieve more precise differentiation; molecular tools were employed, including 16S rRNA gene sequencing and a set of repetitive sequence-based primers such as ERIC, STRR, and HIP. Phylogenetic analyses and the resulting genomic fingerprinting patterns demonstrated that, each strain exhibited a unique profile, distinguishing it from the others. Notably, this study represents the first documented report of genomic fingerprinting at such a level of strain diversity in Iran. The congruence of these findings with the results of the current study, which also utilized the same three groups of primers (ERIC, STRR, and HIP) to identify five strains, underscores the high precision and efficacy of these molecular markers in differentiating closely related phenotypic strains (Shokraei *et al*. 2019).

In the present study, the isolated cyanobacterial strains were clustered into three groups using HIP, STRR, and ERIC primers. The strains *Nostoc* sp. 9, *Aliinostoc* sp. 1, and *Desmonostoc* sp. 10, formed a shared clade, while *Calothrix* sp. 7 and *Neowestiellopsis* sp. 2 frequently constituted distinct branches. The limited number of PCR products generated by the HIP CA primer compared to the other primers may reflect the positional arrangement and orientation of HIP sequences within cyanobacterial genomes. The highest number of amplified bands was observed in *Aliinostoc* sp. 1 and *Calothrix* sp. 7, which may be attributable to the absence of certain PCR products in other strains. The clustering of specific strains within the same clade indicates genetic relatedness that may correspond to the geographic origin of the cyanobacteria.

Overall data analysis revealed that, the combined use of these markers not only enhances genetic resolution but also mitigates the limitations of individual markers. Specifically, the simultaneous application of HIP, STRR, and ERIC enabled more accurate clustering and classification of strains based on genetic similarity. In fact, molecular methods such as rep-PCR with repetitive markers are powerful tools for distinguishing cyanobacterial strains, particularly in natural environments.

Conclusion

In the present study, five cyanobacterial strains isolated for the first time from the Alma-Gol wetland were subjected in detailed morphological, molecular, and phylogenetic analyses. Considering that, cyanobacteria are producers of a wide range of bioactive secondary metabolites, yet phylogenetic and genetic diversity studies on them, especially in Iranian ecosystems, have been relatively scarce. This research constitutes a significant step toward the accurate identification and genetic characterization of these microorganisms. In brief, the present study, confirms that, the simultaneous use of structural genes, functional genes, and repetitive genomic markers, alongside bioinformatics analyses, offers a rapid, precise, and scientifically sound approach for the identification, differentiation, and classification of cyanobacteria. The findings of this research lay the groundwork for further studies on biodiversity, identification of potential toxin producer cyanobacteria strains, and the selection of industrial strains with potential for valuable metabolite production. Furthermore, these

insights may contribute to the advancement of environmental management programs, biotechnological applications, and pharmaceutical development in the future.

Given the importance of the subject under study, screening is also recommended during other seasons of the year. Additionally, it would be beneficial to identify other toxic genes responsible for producing toxins such as nodularin, which are highly toxic and lethal, and to extract and quantify these toxins using appropriate analytical instruments such as HPLC and real time PCR. In fact, the amount of toxin produced by each strain can serve as a warning to the indigenous people living in the affected area.

Acknowledgment

This paper is derived from the MSc thesis of the 1st author supervised by the 4th author at the SR.C., Islamic Azad University (Tehran, Iran). The authors gratefully acknowledge the Islamic Azad University authorities for providing laboratory facilities.

References

Akoijam, C. & Singh, A.K. 2011. Molecular typing and distribution of filamentous heterocystous cyanobacteria isolated from two distinctly located regions in North-Eastern India. World Journal of Microbiology and Biotechnology 27(3): 2187–2194. DOI: 10.1007/s11274-011-0684-8.

Baptista, M., Cunha, J.T. & Domingues, L. 2021. DNA-based approaches for dairy products authentication: A review and perspectives. Trends in Food Science & Technology 109(2): 386–397. DOI: 10.1016/j.tifs.2021.01.043.

Becerra-Absalón, I., Rodarte, B., Osorio, K., Alba-Lois, L., Segal-Kischinevzky, C. & Montejano, G. 2013. A new species of *Brasilonema* (Scytonemataceae, Cyanoprokaryota) from Tolantongo, Hidalgo, Central Mexico. Fottea 13(5): 25–38. DOI: 10.5507/fot.2013.003.

Bittner, M., Štern, A., Smutná, M., Hilscherová, K. & Žegura, B. 2021. Cytotoxic and genotoxic effects of cyanobacterial and algal extracts-Microcystin and retinoic acid content. Toxins 13(1): 107–121. DOI: 10.3390/toxins13020107.

Cai, F., Peng, X. & Li, R. 2020. *Violetonostoc minutum* gen. et sp. nov. (Nostocales, Cyanobacteria) from a rocky substrate in China. Algae 35(2): 1–15. DOI:10.4490/algae.2020.35.3.4.

Chonudomkul, D., Yongmanitchai, W., Theeragool, G., Kawachi, M., Kasai, F., Kaya, K. & Watanabe, M.M. 2004. Morphology, genetic diversity, temperature tolerance and toxicity of *Cylindrospermopsis raciborskii* (Nostocales, Cyanobacteria) strains from Thailand and Japan. FEMS Microbiology Ecology 48(11): 345–355. DOI: 10.1016/j.femsec.2004.02.014.

De Bruijn, F.J. 1992. Use of repetitive (repetitive extragenic palindromic and enterobacterial repetitive intergeneric consensus) sequences and the polymerase chain reaction to fingerprint the genomes of *Rhizobium meliloti* isolates and other soil bacteria. Applied and Environmental Microbiology 58(1): 2180–2187. DOI: 10.1128/aem.58.7.2180-2187.1992.

Desikachary, T.V. 1959. Cyanophyta, New Delhi. Indian Council of Agricultural Research 12(4): 1431–1500. DOI: 10.1007/s10811-012-9793-5.

Fewer, D.P., Rouhiainen, L., Jokela, J., Wahlsten, M., Laakso, K., Wang, H. & Sivonen, K. 2007. Recurrent adenylation domain replacement in the microcystin synthetase gene cluster. BMC Evolutionary Biology 7(4): 1–11. DOI: 10.1186/1471-2148-7-183.

Guajardo-Leiva, S., Pedrós-Alió, C., Salgado, O., Pinto, F. & Díez, B. 2018. Active crossfire between Cyanobacteria and Cyanophages in phototrophic mat communities within hot springs. Frontiers in Microbiology 9(1): 20–39. DOI: 10.3389/fmicb.2018.02039.

Hulton, C., Higgins, C. & Sharp, P. 1991. ERIC sequences: a novel family of repetitive elements in the genomes of *Escherichia coli*, *Salmonella typhimurium* and other enterobacteria. Molecular Microbiology 5(1): 825–834. DOI: 10.1111/j.1365-2958.1991.tb00755.x.

Iteman, I., Rippka, R., Tandeau de Marsac, N. & Herdman, M. 2000. Comparison of conserved structural and regulatory domains within divergent 16S rRNA–23S rRNA spacer sequences of cyanobacteria. Microbiology 146(3): 1275–1286. DOI: 10.1099/00221287-146-6-1275.

Komárek, J. 2006. Cyanobacterial taxonomy: current problems and prospects for the integration of traditional and molecular approaches. Algae 21(2): 349–375. DOI: 10.4490/algae.2006.21.4.349.

Komárek, J., Sant'Anna, C.L., Bohunicka, M., Mareš, J., Hentschke, G.S., Rigonato, J. & Fiore, M.F. 2013. Phenotype diversity and phylogeny of selected *Scytonema* species (Cyanoprokaryota) from SE Brazil. Fottea 13(3): 173–200. DOI: 10.5507/fot.2013.015.

Kotai, J. 1972. Instruction of preparations of modified nutrient medium Z8 for algae. Norw. Institute of Water Research 4(3): 32–39.

Lepère, C., Wilmotte, A. & Meyer, B. 2000. Molecular diversity of Microcystis strains (Cyanophyceae, Chroococcales) based on 16S rDNA sequences. Systematics and Geography of Plants 4(4): 275–283. DOI: 10.2307/3668646.

Mutoti, M., Gumbo, J. & Jideani, A.I.O. 2022. Occurrence of cyanobacteria in water used for food production: A review. Physics and Chemistry of the Earth, Parts A/B/C 125(2): 103–121. DOI: 10.1016/j.pce.2021.103101.

Neilan, B., Saker, M., Fastner, J., Törökné, A. & Burns, B. 2003. Phylogeography of the invasive cyanobacterium *Cylindrospermopsis raciborskii*. Molecular Ecology 12(1): 133–140. DOI: 10.1046/j.1365-294X.2003.01709.x.

Neilan, B.A., Jacobs, D., Therese, D.D., Blackall, L.L., Hawkins, P.R., Cox, P.T. & Goodman, A.E. 1997. rRNA sequences and evolutionary relationships among toxic and nontoxic cyanobacteria of the genus *Microcystis*. International Journal of Systematic and Evolutionary Microbiology 47(4): 693–697. DOI: 10.1099/00207713-47-3-693.

Nowruzi, B., Becerra-Absalón, I. & Metcalf, J.S. 2023. A novel microcystin-producing cyanobacterial species from the genus *Desmonostoc*, *D. alborizicum* sp. nov., isolated from a water supply system of Iran. Current Microbiology 80(1): 49–53. DOI: 10.1007/s00284-022-03144-5.

Nowruzi, B. & Beiranvand, H. 2024. In vitro and in vivo study of the antifungal activity of extracellular products of cyanobacterium *Neowestiellopsis persica* strain A1387 against *Fusarium* wilt disease of cucumber. Revista Argentina de Microbiología 57(3): 182–197. DOI: 10.1016/j.ram.2024.10.011.

Nowruzi, B., Beiranvand, H., Aghdam, F.M. & Barandak, R. 2024. The effect of plasma activated water on antimicrobial activity of silver nanoparticles biosynthesized by cyanobacterium *Alborzia kermanshahica*. BMC Biotechnology 24(2): 75–93. DOI: 10.1186/s12896-024-00905-x.

Nowruzi, B., Blanco, S. & Nejadsattari, T.J.I.J.O.A. 2018. Chemical and Molecular Evidences for the Poisoning of a Duck by Anatoxin-a, Nodularin and Cryptophycin at the Coast of Lake Shoormast (Mazandaran Province, Iran). International Journal on Algae 20(1): 41–58. DOI: 10.1615/InterJAlgae.v20.i4.30.

Nowruzi, B., Bouaïcha, N., Metcalf, J.S., Porzani, S.J. & Konur, O. 2021. Plant-cyanobacteria interactions: Beneficial and harmful effects of cyanobacterial bioactive compounds on soil-plant systems and subsequent risk to animal and human health. Phytochemistry 192(11): 112–159. DOI: 10.1016/j.phytochem.2021.112959.

Nowruzi, B. & Fahimi, H. 2022. Fingerprinting and molecular phylogeny of some heterocystous

cyanobacteria using 16S rRNA, ITS regions and highly iterated palindromes as molecular markers. Rostaniha 23(2): 79–104. DOI: 10.22092/BOTANY.2022.358594.1306.

Nowruzi, B. & Hutarova, L. 2023. Structural and functional genes, and highly repetitive sequences commonly used in the phylogeny and species concept of the phylum Cyanobacteria. Cryptogamie, Algologie 44(15): 59–84. DOI: 10.5252/cryptogamie-algologie2023v44a3.

Nowruzi, B., Khavari-Nejad, R.-A., Sivonen, K., Kazemi, B., Najafi, F. & Nejadsattari, T. 2012. Identification and toxigenic potential of a *Nostoc* sp. Algae 27(12): 303–313. DOI: 10.4490/algae.2012.27.4.303.

Nowruzi, B., Khavari-Nejad, R.A., Sivonen, K., Kazemi, B., Najafi, F. & Nejadsattari, T.J.P.I.B.S. 2013. Identification and toxigenic potential of a cyanobacterial strain (*Stigomena* sp.). Algae 3(2): 79–85. DOI: 10.4490/algae.2012.27.4.303.

Nowruzi, B. & Lorenzi, A.S. 2024. Morphological and molecular characterization of Goleter sp. (Nostocales, Nostocaceae) isolated from freshwater in Iran. Cryptogamie, Algologie 45(1): 39–51. DOI: 10.5252/cryptogamie-algologie2024v45a4.

Nowruzi, B. & Shalygin, S. 2021. Multiple phylogenies reveal a true taxonomic position of *Dulcicalothrix alborzica* sp. nov. (Nostocales, Cyanobacteria). Fottea 21(4): 235–246. DOI: 10.5507/fot.2021.008.

Nowruzi, B. & Soares, F. 2021. *Alborzia kermanshahica* gen. nov., sp. nov. (Chroococcales, Cyanobacteria), isolated from paddy fields in Iran. International Journal of Systematic and Evolutionary Microbiology 71(4): 14–26. DOI: 10.1099/ijsem.0.004828.

Nowruzi, B. & Zakerfirouzabad, M. 2024. Antifungal activity of *Neowestiellopsis persica* against *Rhizoctonia solani* in root and crown of Faba bean cultivated under modified BG-110 medium composition. The Microbe 4(11): 51–71. DOI: 10.1016/j.microb.2024.100112.

Orcutt, K., Rasmussen, U., Webb, E.A., Waterbury, J.B., Gundersen, K. & Bergman, B. 2002. Characterization of *Trichodesmium* spp. by genetic techniques. Applied and Environmental Microbiology 68(13): 2236–2245. DOI: 10.1128/AEM.68.5.2236-2245.2002.

Rantala, A., Rajaniemi-Wacklin, P., Lyra, C., Lepistö, L., Rintala, J., Mankiewicz-Boczek, J. & Sivonen, K. 2006. Detection of microcystin-producing cyanobacteria in Finnish lakes with genus-specific microcystin synthetase gene E (mcyE) PCR and associations with environmental factors. Applied and Environmental Microbiology 72(4): 6101–6110. DOI: 10.1128/AEM.01058-06.

Rasmussen, U. & Svenning, M.M. 1998. Fingerprinting of cyanobacteria based on PCR with primers derived from short and long tandemly repeated repetitive sequences. Applied and Environmental Microbiology 64(3): 265–272. DOI: 10.1128/AEM.64.1.265-272.1998.

Rouhiainen, L., Sivonen, K., Buikema, W.J. & Haselkorn, R. 1995. Characterization of toxin-producing cyanobacteria by using an oligonucleotide probe containing a tandemly repeated heptamer. Journal of Bacteriology 177(15): 6021–6026. DOI: 10.1128/jb.177.20.6021-6026.1995.

Sánchez-Baracaldo, P., Bianchini, G., Wilson, J.D. & Knoll, A.H. 2022. Cyanobacteria and biogeochemical cycles through earth history. Trends in Microbiology 30(17): 143–157. DOI: 10.1016/j.tim.2021.05.008.

Selvakumar, G. & Gopalaswamy, G. 2008. PCR based fingerprinting of *Westiellopsis* cultures with short tandemly repeated repetitive (STRR) and highly iterated palindrome (HIP) sequences. Biologia 63(2): 283–288. DOI: 10.2478/s11756-008-0065-4.

Shokraei, R., Fahimi, H., Blanco, S. & Nowruzi, B. 2019. Genomic fingerprinting using highly repetitive

sequences to differentiate close cyanobacterial strains. Microbial Bioactivity 2(13): 068–075. DOI: 10.25163/microbbioacts.21015A2624310119.

Singh, P., Kaushik, M.S., Srivastava, M. & Mishra, A.K. 2014. Phylogenetic analysis of heterocystous cyanobacteria (Subsections IV and V) using highly iterated palindromes as molecular markers. Physiology and Molecular Biology of Plants 20(5): 331–342. DOI: 10.1007/s12298-014-0244-4.

Smith, J., Parry, J., Day, J. & Smith, R. 1998. A PCR technique based on the Hipl interspersed repetitive sequence distinguishes cyanobacterial species and strains. Microbiology 144(34): 2791–2801. DOI: 10.1099/00221287-144-10-2791.

Tavakoli, Y., Mohammadipanah, F., Te, S.H., You, L. & Gin, K.Y.-H. 2021. Biodiversity, phylogeny and toxin production profile of cyanobacterial strains isolated from lake Latyan in Iran. Harmful Algae 106(10): 102–154. DOI: 10.1016/j.hal.2021.102054.

Valerio, E., Chambel, L., Paulino, S., Faria, N., Pereira, P. & Tenreiro, R. 2009. Molecular identification, typing and traceability of cyanobacteria from freshwater reservoirs. Microbiology 155(4): 642–656. DOI: 10.1099/mic.0.022848-0.

Wilson, A.E., Sarnelle, O., Neilan, B.A., Salmon, T.P., Gehringer, M.M. & Hay, M.E. 2005. Genetic variation of the bloom-forming cyanobacterium *Microcystis aeruginosa* within and among lakes: implications for harmful algal blooms. Applied and Environmental Microbiology 71(1): 6126–6133. DOI: 10.1128/aem.71.10.6126-6133.2005.

Wilson, K.M., Schembri, M.A., Baker, P.D. & Saint, C.P. 2000. Molecular characterization of the toxic cyanobacterium *Cylindrospermopsis raciborskii* and design of a species-specific PCR. Applied and Environmental Microbiology 66(12): 332–338. DOI: 10.1128/AEM.66.1.332-338.2000.

Zheng, W., Song, T., Bao, X., Bergman, B. & Rasmussen, U. 2002. High cyanobacterial diversity in coralloid roots of cycads revealed by PCR fingerprinting. FEMS Microbiology Ecology 40(6): 215–222. DOI: 10.1111/j.1574-6941.2002.tb00954.x.